Mutual passivation effects in Si-doped diluted $In_yGa_{1-y}As_{1-x}N_x$ alloys

J. Wu,[1,2] K. M. Yu,[1] W. Walukiewicz,[1,*] G. He,[3] E. E. Haller,[1,2] D. E. Mars,[4] and D. R. Chamberlin[4]
[1]*Materials Sciences Division, Lawrence Berkeley National Laboratory, Berkeley, California 94720, USA*
[2]*Department of Materials Science and Engineering, University of California, Berkeley, California 94720, USA*
[3]*Department of Mechanical Engineering, Massachusetts Institute of Technology, Massachusetts 02139, USA*
[4]*Agilent Laboratories, 3500 Deer Creek Road, Palo Alto, California 94304, USA*
(Received 23 July 2003; published 7 November 2003)

We report systematic investigations of the mutual passivation effects of Si hydrogenic donors and isovalent nitrogen in dilute $InGaAs_{1-x}N_x$ alloys. Upon thermal annealing at temperatures above ~650 °C, the Si atoms diffuse assisted by the formation and migration of Ga vacancies. When they find nitrogen atoms, they form stable Si_{Ga}-N_{As} nearest-neighbor pairs. As a result of the pair formation, the electrical activity of Si_{Ga} donors is passivated. At the same time, the effect of an equal number of N_{As} atoms is also deactivated. The passivation of the shallow donors and the N_{As} atoms is manifested in a drastic reduction in the free electron concentration and, simultaneously, an increase in the fundamental band gap. Analytical calculations of the passivation process based on Ga vacancies mediated diffusion show good agreement with the experimental results. Monte Carlo simulations have also been performed for a comparison with these results. The effects of mutual passivation on the mobility of free electrons are quantitatively explained on the basis of the band anticrossing model. Optical properties of annealed Si-doped $InGaAs_{1-x}N_x$ samples are also discussed.

DOI: 10.1103/PhysRevB.68.195202 PACS number(s): 71.20.Nr, 61.72.Ss, 66.30.−h

I. INTRODUCTION

It has been discovered recently that the electronic properties of some compound semiconductor alloys are greatly affected by the substitution of a small fraction of metallic anions with electronegative isovalent atoms. Group III-V-N materials, in which the highly electronegative N atoms partially substitute for more metallic anions in standard III-V compounds, is the most representative and extensively studied class of such highly mismatched alloys (HMAs).[1] In close analogy, partial substitution of group VI anions by electronegative O in II-VI compounds leads to the formation of group II-VI-O HMAs.[2] It has been shown that in both cases the incorporation of the highly electronegative anions modifies the electronic structure of the conduction band through an anticrossing interaction between the localized acceptorlike states of the electronegative atoms and the extended conduction band states of the semiconductor matrix.[1,2] On the other hand, a partial substitution of electronegative anions with more metallic isovalent atoms leads to a modification of the valence band structure through the anticrossing interaction between the localized donorlike states of the metallic atoms and the extended states of the valence band of the semiconductor matrix. The valence band anticrossing effects were recently observed in Se- and S-rich $ZnSe_{1-x}Te_x$ and $ZnS_{1-x}Te_x$ alloys.[3,4]

It has been shown that the modification of the electronic structure has a dramatic effect on the electrical activity of the donor dopants in InGaAsN. An enhancement of more than an order of magnitude in the maximum achievable free electron concentration has been demonstrated in $GaAs_{1-x}N_x$ thin films doped with group VI donors (Se and S).[5,6] However, doping the material with group IV donors (Si) results in highly resistive $GaAs_{1-x}N_x$.[7] The failure to activate the Si donors in GaAsN alloys has been explained by the mutual passivation of Si shallow donors and isovalent N impurities.[8] While a high electron concentration is achieved in Si-doped InGaAsN grown by molecular beam epitaxy at relatively low temperature (~400 °C), during high temperature annealing, the Si donor diffuses on the Ga sublattice until it forms a nearest-neighbor pair with a N_{As} atom. The formation of the Si-N pair deactivates the electrical activities of both species. As a result the free electron concentration decreases rapidly with high temperature annealing accompanied by an increase in the fundamental band gap. In contrast group VI donors such as Se or S do not show such a mutual passivation effect in $GaAs_{1-x}N_x$ because they share the same anion sublattice with N, and therefore cannot form nearest-neighbor pairs with N. Polimeni *et al.* have shown that the introduction of hydrogen into $GaAs_{1-x}N_x$ thin films and quantum wells leads to the formation of N-H bonds that results in the passivation of N.[9] Subsequent thermal annealing up to 550 °C dissociates the N-H bond, completely restoring the band gaps of the nitride layers to their values prior to hydrogenation. The effects of hydrogenation in this material are very similar to the well-known H passivation of electrically active dopants in semiconductors.[10] On the other hand, the formation of Si-N bonds in the $GaAs_{1-x}N_x$:Si system results in the mutual passivation of the Si atoms as shallow donors and the N atoms as isovalent impurities. These mutual passivation effects are thermally stable up to 950 °C.

In this paper we present systematic studies of the mutual passivation effect in Si-doped $In_yGa_{1-y}As_{1-x}N_x$ alloys. We derive the diffusion equation of Si donors, taking into account both the Fermi-level independent (neutral vacancy mediated) and Fermi-level dependent (charged vacancy mediated) diffusion mechanisms. The resultant analytical equation and Monte Carlo simulation show good agreement with the measured electron concentration. The effect of thermal anneal on the mobility of free electrons is also studied. Optical properties have also been measured and the results are discussed.

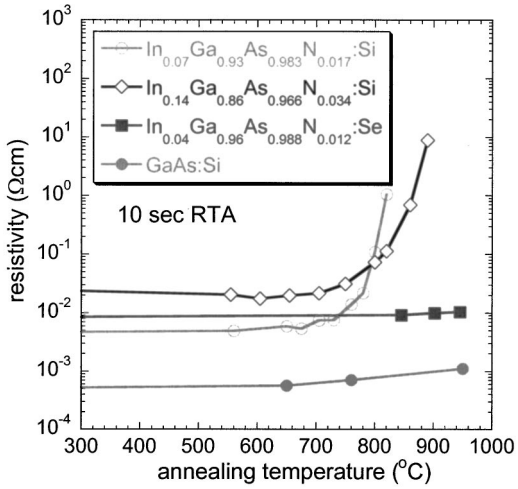

FIG. 1. Resistivity changes with a 10-sec anneal over a wide range of temperatures. The total Si concentration is about 9×10^{19} cm^{-3} in both InGaAsN:Si samples, and is about 1.6×10^{19} cm^{-3} in the GaAs:Si sample. The Se concentration in the InGaAsN:Se sample is about 4×10^{20} cm^{-3}.

II. EXPERIMENT

$In_yGa_{1-y}As_{1-x}N_x$ layers with thickness of ~0.5 μm were grown by molecular beam epitaxy (MBE) on semi-insulating GaAs substrates at a substrate temperature of $\sim$450 °C. Indium was introduced to compensate for the N-induced lattice contraction, improving the crystal quality by making it lattice matched to the GaAs substrate. Si dopants were introduced during the growth. The epitaxially grown samples were rapid thermally annealed (RTA) in a flowing N_2 ambient in the temperature range of 550–950 °C for 10–120 s with the sample surface protected by a blank GaAs wafer. The resistivity, free electron concentration and mobility were measured by Hall effect experiments in the Van de Pauw geometry.

The band gaps of the films were measured by photomodulated reflectance (PR) spectroscopy at room temperature using a chopped HeCd laser beam (wavelength 442 nm) for modulation. The photoluminescence (PL) signals were generated in the backscattering geometry by excitation with the 515-nm line of an argon laser. The signals were then dispersed by a SPEX 1680B monochromator and detected by a liquid-nitrogen-cooled Ge photodiode.

III. MUTUAL PASSIVATION

A. Experimental results

Figure 1 shows the results of resistivity measurements of a series of Si-doped $In_yGa_{1-y}As_{1-x}N_x$ and GaAs films after RTA for 10 sec in the temperature range of 550–950 °C. From the growth conditions of the InGaAsN:Si samples the Si concentration has been estimated to be $\sim9\times10^{19}$ cm^{-3}. For the GaAs:Si film without N, only a slight increase in the resistivity is observed as the RTA temperature increases, corresponding to a decrease in electron concentration (n) from 1.6×10^{19} to 8×10^{18} cm^{-3}. As pointed out in Ref. 8, such a decrease of electron concentration in GaAs is the result of thermal annealing that drives the system to an equilibrium state with the saturated electron concentration of $\sim10^{19}$ cm^{-3}.[11]

In stark contrast to the behavior of the GaAs:Si thin film, the resistivity of both $In_yGa_{1-y}As_{1-x}N_xSi$ films rises rapidly at RTA temperatures higher than about 700 °C. The rise in the resistivity corresponds to reduction in the electron concentration from $\sim10^{19}$ cm^{-3} in the as-grown films to $\sim10^{17}$ cm^{-3} in the films after RTA at 950 °C. RTA of the $In_yGa_{1-y}As_{1-x}N_x$:Si sample at 950 °C for longer time further reduces the free electron concentration in the samples (to $<10^{15}$ cm^{-3} for 120-sec RTA) while no significant change is observed in the GaAs:Si sample.

In $In_yGa_{1-y}As_{1-x}N_x$ crystals grown at relatively low temperatures ($\sim$400 °C) by MBE, Si and N atoms are randomly distributed on Ga and As sublattice sites, respectively (a small fraction of Si are also expected to occupy As sites). The diffusion activation energy for Si in highly n-type doped GaAs is $\sim$2.5 eV,[12] which is much lower than the activation energy for N diffusion in GaAs [$\sim$3.6 eV (Ref. 13)]. Therefore, we can neglect the diffusion of N in the RTA temperature range used in this study. Upon RTA, sufficiently high thermal energy is supplied for Si atoms to diffuse in the crystal to reach lower energy positions. Since N is much more electronegative than As,[14] the Si-N bond is expected to be much stronger than the Si-As bond.[15] Therefore, anyone of the four nearest-neighboring Ga sites of the N_{As} atoms becomes an effective trap for the diffusing Si atoms. As a result of the Si_{Ga}-N_{As} pair formation, the fourth valence electron of the Si atom is locally bound to the N atom as opposed to being donated to the conduction band. Consequently the electrical activity of Si as a hydrogenic donor in InGaAsN is passivated. This explanation is further supported by the fact that group VI doped (In)$GaAs_{1-x}N_x$ alloys do not show such donor passivation behavior upon RTA.[8] As shown in Fig. 1, only a small decrease of electron concentration is observed in the Se-doped $In_yGa_{1-y}As_{1-x}N_x$ thin film after annealing at 950 °C, similar to the behavior of the GaAs:Si sample. The reason for this different behavior is that group VI atoms act as shallow donors only when they reside on the As sublattice (group V) sites. Therefore they cannot form nearest neighbor pair bonds with N_{As} atoms.

Shown in Fig. 2 are the PR spectra of three samples after different isothermal anneals. The annealing temperature and time are shown along each curve. The band gap has been determined from fitting the spectra with the standard third-derivative functional form.[16] The inset shows the band gap as a function of the annealing temperature, along with the active nitrogen mole fraction calculated from the band gap using the band anticrossing model [Eq. (11)]. The bandgap energy is increasing with increasing annealing temperature. If the increase is solely attributed to deactivation of the N atoms the concentration of the deactivated N is approximately equal to $0.004\times2.2\times10^{22}$ cm$^{-3}\sim8\times10^{19}$ cm^{-3}, i.e., close to the initial total Si concentration in the as-grown sample. This is consistent with the picture that the formation of Si_{Ga}-N_{As} pairs is responsible for the mutual passivation of both species. It passivates the electrical activity of Si donors and deactivates N as the isovalent dopant. The nitrogen de-

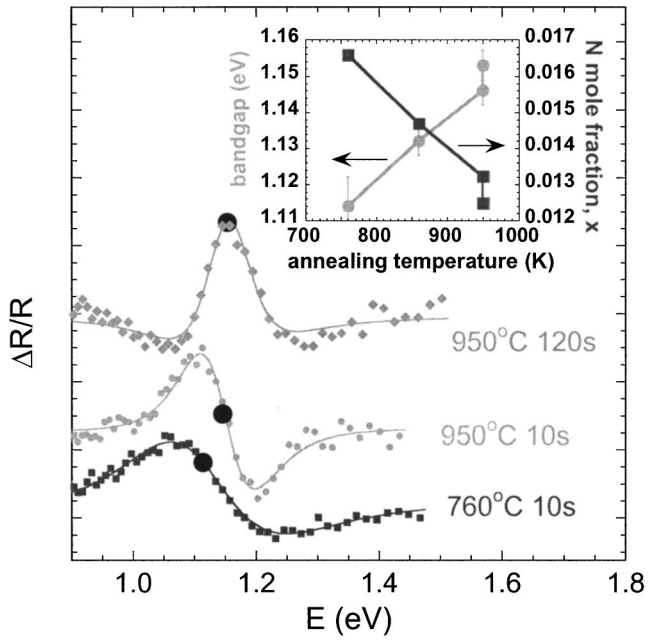

FIG. 2. PR spectra of $In_{0.07}Ga_{0.93}As_{0.983}N_{0.017}$ samples with different isothermal anneals. The black dots in each curve indicate the band-gap energies obtained by fitting the standard third derivative equation (Ref. 16) to the experimental data. Inset: the band-gap energies and active N mole fraction estimated from the BAC model plotted as a function of the annealing temperature.

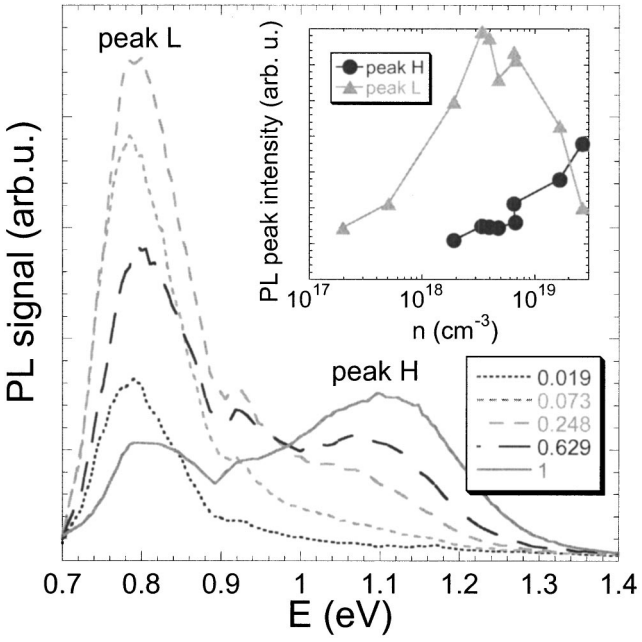

FIG. 3. PL spectra of several $In_{0.07}Ga_{0.93}As_{0.983}N_{0.017}$ samples with different anneals. The normalized free electron concentration for each spectrum is indicated in the legend. Inset: the intensity of the two PL peaks as a function of electron concentration.

activation effect can be better resolved in samples in which the initial N concentration and the Si concentration are approximately equal. We have demonstrated this by introducing high concentrations of Si and N into GaAs by ion implantation followed by pulsed laser melting and rapid thermal annealing treatments.[8] It was shown that the active N concentration in a Si and N coimplanted sample is lower than that in an N-alone implanted sample (implanted with the same N dose) by an amount that is approximately equal to the total Si concentration.

The Si_{Ga}-N_{As} pair strongly binds the fourth valence electron of Si transforming this hydrogenic donor into a deep localized center. In Fig. 3 we show the PL spectra from a series of Si-doped $In_{0.07}Ga_{0.93}As_{0.983}N_{0.017}$ samples annealed at different temperatures. Two peaks are clearly observed in the spectra. The higher energy PL peak (peak *H*) at 1.1 eV corresponds to the band-to-band transitions. With reduced electron concentration, this peak gradually disappears, possibly due to increasing concentration of unknown nonradiative recombination defects generated by the high temperature annealing.

A deep-level related broad peak (peak *L*) is observed at an energy of about 0.8 eV. As shown in the inset of Fig. 3 the intensity of this peak exhibits a nonmonotonic dependence on the electron concentration. We tentatively attribute peak *L* to optical transitions involving states associated with the Si-N pairs. As the concentration of Si-N pairs increases with decreasing *n*, the emission intensity is enhanced. Upon further annealing, nonradiative transitions start to dominate the recombination process; as a result the intensities of both peak *H* and peak *L* vanish gradually.

B. Theory

In order to elucidate the microscopic nature of the passivation process we consider the diffusion of substitutional Si atoms in InGaAsN alloys. Yu *et al.*[17] and Ahlgren *et al.*[18] have shown that the diffusion of Si in GaAs involves the formation and migration of neutral Ga vacancies (V_{Ga}^{0}), triply negatively charged Ga vacancies (V_{Ga}^{3-}) and As vacancies (V_{As}). In our case only the Si atoms on the Ga sublattice contribute to the mutual passivation; therefore we consider the first two mechanisms in the model. The diffusion coefficient of Si on the Ga sublattice in GaAs is the combination of the Fermi-level independent term (mainly via V_{Ga}^{0}) and the Fermi-level dependent term (via V_{Ga}^{3-}),

$$D(T,t)=D^{0}(T)+D^{\alpha-}(T)\cdot\left[\frac{n(t)}{n_i}\right]^{\alpha}, \tag{1}$$

where $D^{0}(T)=D_0^{0}\exp[-E_a^{0}/k_BT]$, $D^{\alpha-}(T)=D_0^{\alpha-}\times\exp[-E_a^{\alpha-}/k_BT]$, and $\alpha=3$ is the negative charge state of V_{Ga}^{3-}. The intrinsic carrier concentration in semiconductors can be written as

$$n_i\approx B\cdot T^{3/2}\exp\left[-\frac{E_g'}{2k_BT}\right], \tag{2}$$

where

$$B \equiv 2[\sqrt{m_e^* m_h^*} k_B/2\pi\hbar^2]^{3/2} \exp(\gamma/2k_B) \tag{3}$$

is a constant depending on the free carrier effective masses and the linear temperature coefficient of the direct band gap (γ), but nearly independent of temperature. E_g' is an "effective band gap" that takes into account the contributions of the electron density of states near the X and L points as well as the Γ point in the band structure.[19] The diffusion coefficient can be rewritten as

$$D(T,t) = g(T)\left\{ r(T) + \left[\frac{n(t)}{n_0}\right]^{\alpha}\right\}, \tag{4}$$

where

$$g(T) \equiv D_0^{\alpha-} \exp\left[-\frac{E_a^{\alpha-}}{k_B T}\right]\left[\frac{n_0}{n_i}\right]^{\alpha} \tag{5a}$$

is the V_{Ga}^{3-} mediated diffusion coefficient at time $t=0$, and

$$r(T) \equiv \frac{D^0(T)}{g(T)} = \frac{D_0^0}{D_0^{\alpha-}} \exp\left[-\frac{E_a^0 - E_a^{\alpha-}}{k_B T}\right]\left[\frac{n_i}{n_0}\right]^{\alpha} \tag{5b}$$

is the ratio of the V_{Ga}^0 mediated and the V_{Ga}^{3-} mediated diffusion coefficients.

For random walk on a face-centered-cubic sublattice, our Monte Carlo simulation has shown that the total number of As sublattice sites that is nearest neighboring a Ga site that the "walker" has visited is directly proportional to the diffusion time multiplied by the diffusion coefficient. This number (L) is also proportional to the diffusion length to the power of 2, which is a well-known result from the random walk theory.

We assume that $D(T,t)$ is a slowly varying function that can be treated as a constant within a short period of time dt. According to the mutual passivation mechanism, the reduction rate of $\mathrm{Si_{Ga}}$ (hence of the free electron concentration n) is proportional to the total number of active nitrogen atoms residing in the diffusion volume,

$$\frac{dn(t)}{n(t)} = -x dL(t) \propto x \frac{D(T,t)}{a^2} dt. \tag{6}$$

In this equation a is the distance between nearest neighbors on the Ga sublattice, and x is the mole fraction of active N atoms. Since [N] is much larger than [Si] in our $\mathrm{InGaAs_{1-x}N_x}$:Si samples, we neglect the passivation of N caused by the Si-N pair formation, and replace x in Eq. (6) by the initial N fraction (x_0). Equations (4) and (6) lead to the differential equation

$$\frac{dn}{n\cdot[r(T) + (n/n_0)^{\alpha}]} = -\frac{\beta x_0 g(T) dt}{a^2}, \tag{7}$$

where β is a constant that is proportional to the Si passivation rate. The solution is

$$\ln\left[\frac{n(t)}{n_0}\right] = -\frac{1}{\alpha}\ln\left\{\left(1 + \frac{1}{r(T)}\right)\exp\left[\frac{\alpha\beta x_0 D^0(T)}{a^2} t\right] - \frac{1}{r(T)}\right\}. \tag{8}$$

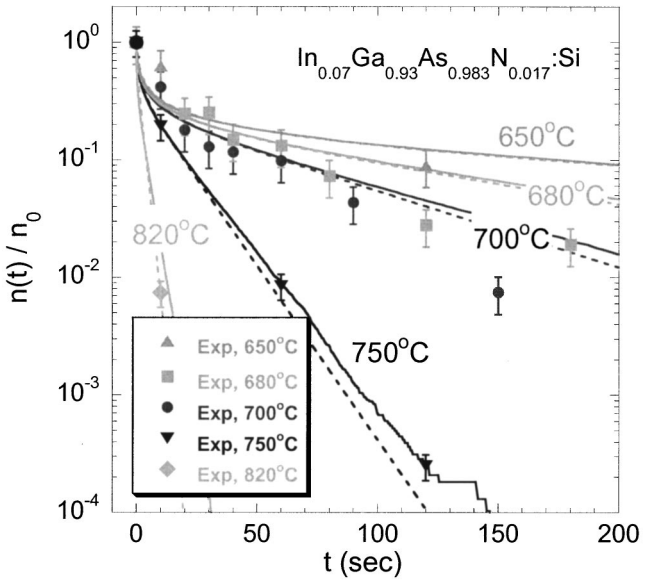

FIG. 4. Normalized free electron concentration (log scale) as a function of annealing time at different annealing temperatures. The solid and dashed curves represent the results from the Monte Carlo simulation and the analytical calculation [Eq. (8)], respectively.

At $r \gg 1$ (high temperatures), Eq. (8) becomes

$$n(t) \approx n_0 \exp\left[-\frac{\beta x_0 D^0(T)}{a^2} t\right], \tag{9}$$

i.e., $\ln[n(t)/n_0]$ is linear in t, where the slope is determined by the V_{Ga}^0-mediated Si diffusion.

At long times t, Eq. (8) can be simplified

$$n(t) \approx n_0\left[1 + \frac{1}{r(T)}\right]^{-1/\alpha} \exp\left[-\frac{\beta x_0 D^0(T)}{a^2} t\right], \tag{10}$$

i.e., $\ln[n(t)/n_0]$ approaches a similar linear dependence on t, with the reduction rate of $n(t)$ also dominated by the Si diffusion through V_{Ga}^0.

C. Comparison between theory and experiments

As shown in the preceding section, the V_{Ga}^{3-}-mediated diffusion of Si strongly depends on the Fermi level and thus also on the electron concentration which in turn is equal to the concentration of electrically active, unpassivated $\mathrm{Si_{Ga}}$ atoms. This leads to a dynamical diffusion process that has a self-consistent solution given by Eq. (8).

Comparisons between our experimental results on the annealing effects of the electrical properties of Si-doped InGaAsN alloys and our theoretical analysis are presented in Figs. 4 and 5. Figures 4 and 5 show the isothermal and isochronal annealing effects, respectively, of the free carrier concentration of a $\mathrm{In_{0.07}Ga_{0.93}As_{0.983}N_{0.017}Si}$ sample with $[\mathrm{Si}] \sim 9\times10^{19}\ \mathrm{cm}^{-3}$ for annealing temperature in the range of 650–820 °C. The results of calculations based on Eq. (8) are shown as dashed lines in Figs. 4 and 5. According to the diffusion model, at high annealing temperatures or long annealing time, the Fermi-level independent, V_{Ga}^0-mediated dif-

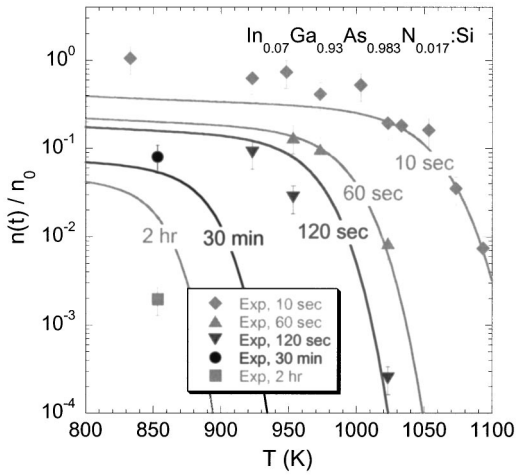

FIG. 5. Normalized free electron concentration (log scale) as a function of annealing temperature with different annealing time. The solid curves represent the results from the analytical calculation [Eq. (8)].

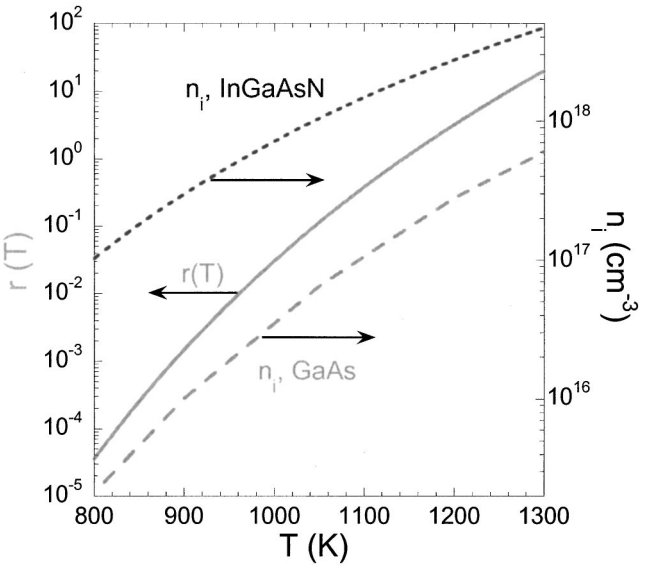

FIG. 6. Temperature dependence of the ratio (r) between the Fermi-level independent and dependent diffusion coefficients at initial electron concentration. Also shown are the calculated intrinsic electron concentration of GaAs (from Ref. 19) and of our InGaAsN sample.

fusion becomes increasingly important. This is reflected in the fact that the $\ln[n/n_0]\sim t$ curves approach a linear dependence at high temperatures or long anneal times, in which the slope is determined by the constant V_{Ga}^0-mediated diffusion coefficient.

Notice in Fig. 5, for 10-s isochronal annealing, the electron concentration starts to decrease rapidly at ~700 °C. This onset temperature roughly corresponds to the annealing condition that allows the Si atoms to diffuse over a length equal to the average distance between randomly distributed Si and N atoms (~7 Å). With increasing annealing time, this onset shifts to lower temperatures. With 2-h furnace annealing at temperatures as low as 580 °C, more than two decades of drop in n was observed. Calculations based on Eq. (8) at these annealing times show good agreement with experiments. The deviation at low temperatures for the 10-s anneal can be attributed to the presence of the relatively high concentration of $\mathrm{Si_{As}}$, and interstitial Si atoms in the beginning[18] that transfer to $\mathrm{Si_{Ga}}$ when $\mathrm{Si_{Ga}}$ starts to be passivated.

The various parameters used in our calculations are summarized in Table I. We note that, as shown in Table I, we use only two adjustable parameters: β, that describes the passivation rate of Si in the diffusion process, and B, that is introduced in Eq. (2) to describe the intrinsic carrier concentration (n_i) in $\mathrm{InGaAs_{1-x}N_x}$. All the other parameters, such as the prefactors and activation energies of V_{Ga}^0- and V_{Ga}^{3-}-mediated diffusion are adopted from Ref. 18. The temperature dependence of n_i for GaAs listed by Blakemore[19] can be well described by Eq. (2) with $B=4.37\times10^{16}\ \mathrm{cm^{-3}\,K^{-3/2}}$. These n_i data are plotted in Fig. 6. The best-fit constant B in our InGaAsN:Si sample is smaller by a factor of 0.32 than that of GaAs. This is reasonably close to the rescaling factor of 0.24 obtained by simply replacing $m_e^*=0.067m_0$ and $\gamma=0.5$ meV/K for GaAs in Eq. (3) with values for $\mathrm{In_{0.07}Ga_{0.93}As_{0.983}N_{0.017}}$: $m_e^*\approx0.1m_0$ (Refs. 1 and 20) and $\gamma\approx0.2$ meV/K.[21] The small discrepancy can be attributed to the enhanced electron effective mass in InGaAsN alloys at high doping levels.[20] Also, as can be seen from Eqs. (5b) and (2), B enters the final fitting equation in a product with the prefactors of the diffusion coefficients (D_0^0 and $D_0^{\alpha-}$). Therefore, the change in B could be also attributed to the changes of D_0^0 and $D_0^{\alpha-}$ in our InGaAsN sample as compared with the values of these parameters for GaAs.[18]

To further understand the diffusion-passivation process, we have performed a Monte Carlo simulation of atoms diffusing on the face-centered-cubic (fcc) sublattice of a zinc-blende structure. We construct a supercell consisting of $200\times200\times200$ cubic unit cells, each containing four Ga sites and four As sites in a zinc-blende coordination. Periodic boundary conditions are applied in all three dimensions. The nitrogen atoms are distributed randomly at appropriate concentrations on the As sublattice. The Si atom is allowed to perform a random walk on the Ga sublattice. Once the Si atom finds an unpaired N atom on one of its nearest-neighboring sites, a permanent Si-N pair is formed with a given probability (defined as the "passivation rate" $\leqslant1$) and

TABLE I. Parameters used in the calculation.

Parameter	β	B ($\mathrm{cm^{-3}\,K^{-3/2}}$)	α	D_0^0 ($\mathrm{Å^2/s}$)	E_a^0 (eV)	$D_0^{\alpha-}$ ($\mathrm{Å^2/s}$)	$E_a^{\alpha-}$ (eV)
value	11	1.4×10^{16}	3	3.74×10^{13}	2.60	5.92×10^{8}	2.28
note		optimized			adopted from Ref. 18		

the donor activity of the Si atom vanishes. Both the Fermi-level dependent and independent diffusion coefficients were included to convert the number of diffusion steps into real diffusion time. The constant β has been determined to be about 10.2 by the simulation assuming a passivation rate of 1. This number is quite close to $\beta=11$ obtained by fitting Eq. (8) with our experimental data. As mentioned before, since β appears only in the product with x_0 and D_0^0 in Eq. (8), the determination of β in the fitting is affected by the uncertainty of x_0 and D_0^0. The internal supplies of Si donors by transferring Si_{As} to the Ga sublattice and the possible dissociation of Si-N pairs at high temperatures could also result in an apparent change in β. The results of the Monte Carlo simulation are shown as solid curves in Fig. 4. The good agreement of both the simulation results and the analytical calculation with the experimental data indicates that the Si_{Ga}-N_{As} pair formation is indeed responsible for the passivation of Si donors.

As shown in Sec. III B, at long annealing times, the diffusion process is dominated by the Fermi-level independent, V_{Ga}^0-mediated mechanism, because the V_{Ga}^{3-}-mediated diffusion is strongly retarded by the decrease of the Fermi level. The larger activation energy of the Fermi-level independent term means a stronger temperature dependence as compared to the Fermi-level dependent term. Accordingly, the relative contribution of V_{Ga}^0-mediated diffusion becomes increasingly important at higher annealing temperatures. The ratio $[r(T)]$ of the Fermi level dependent and the Fermi level independent diffusion coefficients [Eq. 5(b)] at time $t=0$ is shown in Fig. 6 as a function of temperature. It can be seen that at $\sim$870 °C the Fermi-level independent term starts to dominate. As a result $\ln[n(t)/n_0]$ varies linearly with time t from the beginning of the annealing process at these temperatures.

IV. ELECTRONIC TRANSPORT PROPERTIES

The results shown in Fig. 4 indicate that mutual passivation can be used to precisely control the electron concentration over a wide range. This provides an interesting opportunity to study the concentration dependence of the electron mobility in material with the same composition. It has been widely recognized that the incorporation of small amounts of nitrogen into GaAs leads to a drastic reduction of the electron mobility. The typical mobility of $GaAs_{1-x}N_x$ films ranges from $\sim$10 to a few hundred $cm^2/V\,s$,[22,23] which is over an order of magnitude smaller than the electron mobility in GaAs at comparable doping levels.[19] Figure 7 shows the change in room-temperature mobility of $In_{0.07}Ga_{0.93}As_{0.983}N_{0.017}Si$ when the electron concentration is reduced by rapid thermal annealing due to Si_{Ga}-N_{As} formation. The mobility shows a nonmonotonic dependence on the electron concentration with a maximum at $n\sim5\times10^{18}\ cm^{-3}$.

It is now well established that the electronic structure of the conduction band of diluted (In)$GaAs_{1-x}N_x$ alloys is described by the band anticrossing (BAC) model.[1,24] In the BAC model, the conduction band is restructured as a result of an anticrossing interaction between the highly localized states of the isovalent N atoms and the extended states of the host semiconductor (In)GaAs. The newly formed two subbands, named E_+ and E_-, have nonparabolic dispersion relations given by[1]

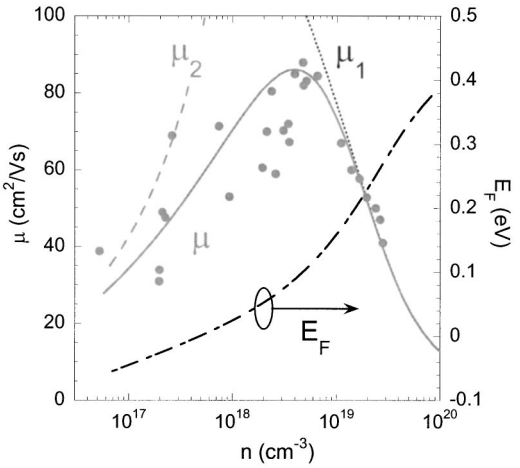

FIG. 7. Room-temperature electron mobility of $In_{0.07}Ga_{0.93}As_{0.983}N_{0.017}$: Si plotted as a function of electron concentration. The calculated mobilities limited by the conduction band broadening (μ_1) and by the random field scattering (μ_2) are shown. The calculated Fermi energy is referenced to the bottom of the lowest conduction band (E_-).

$$E_\pm(\mathbf{k})=\frac{1}{2}\{[E^C(\mathbf{k})+E^L]\pm\sqrt{[E^C(\mathbf{k})-E^L]^2+4V^2x}\}, \tag{11}$$

where $E^C(\mathbf{k})$ is the energy dispersion of the lowest conduction band of the host, and E^L is the energy of the localized states derived from the substitutional N atoms (located at $\sim$0.23 eV above the conduction band edge of GaAs). The coupling between the localized states and the band states of the host is characterized by the parameter V, which has been determined to be 2.7 eV in (In)$GaAs_{1-x}N_x$. The BAC model provides a simple, analytical expression to calculate the electronic and optical properties of diluted (In)$GaAs_{1-x}N_x$ alloys. Numerous effects, including the strong reduction in the fundamental band gap,[1] the increase in the electron effective mass[25] and the hydrostatic pressure dependence of the band gap[24] have been quantitatively explained by the BAC model.

The two-level BAC model is a natural result of degenerate perturbation theory applied to a system comprising localized states and extended states. By using the Green's function method, we have shown that the two-level BAC model [Eq. (11)] can be derived from the Hamiltonian of the many-impurity Anderson model that considers the hybridization of extended states and dilute localized states.[1,26] The imaginary part of the Green's function also provides new information about the electron state broadening that can be used to determine the width of optical transitions and to calculate the free electron mobility. The broadening of the E_- subband is proportional to the admixture of the localized states ($|E^L\rangle$) to the wave function of the restructured states [$|E_-(\mathbf{k})\rangle$],[26]

$$\Gamma_-(\mathbf{k})=|\langle E^L|E_-(\mathbf{k})\rangle|^2\Gamma_L, \tag{12}$$

where $\Gamma_L = \pi V^2 \rho_0(E^L)$ is the level broadening caused by the hybridization obtained in the original single-impurity Anderson model [$\rho_0(E^L)$ is the unperturbed density of states of $E^C(\mathbf{k})$ evaluated at E^L].[27] The broadening defines a finite lifetime for $|E_-(\mathbf{k})\rangle$ through the uncertainty principle, which imposes a limit to the mobility of free electrons that conduct current in the lowest conduction band:

$$\mu_1 = \frac{e\tau(k_F)}{m^*_-(\mathbf{k}_F)} \approx \frac{e\hbar}{m^*_-(\mathbf{k}_F)\Gamma_-(\mathbf{k}_F)}. \tag{13}$$

In this equation, the electron effective mass at the Fermi surface [$m^*_-(\mathbf{k}_F)$] can be calculated from the curvature of the dispersion $E_-(\mathbf{k})$ in Eq. (11).[25] The Fermi wave vector ($\mathbf{k}_F$) and Fermi energy (E_F) are determined by the free electron concentration calculated from the density of states of $E_-(\mathbf{k})$,[1]

$$n(E_F) = \int \frac{\rho_-(E)dE}{1+\exp[(E-E_F)/k_BT]}. \tag{14}$$

The room-temperature mobility (μ_1) calculated from Eq. (13) is shown by the short-dashed curve in Fig. 7. Also shown is the Fermi energy as a function of n calculated from Eq. (14). One sees that at high electron concentrations when the Fermi energy approaches the original energy level of N localized states in $In_{0.07}Ga_{0.93}As_{0.983}N_{0.017}$ (located at ~0.30 eV above the conduction band edge of E^C, or 0.54 eV above the conduction band edge of E_-), the mobility is largely suppressed by the strong hybridization between $|E^L\rangle$ and $|E^C(\mathbf{k})\rangle$. At $n = 2\times10^{19}$ cm^{-3}, the energy broadening and scattering lifetime at the Fermi surface are estimated to be 0.25 eV and 3 fs, respectively. The mean free path of free electrons is about 5 Å, which is only a third of the average distance between the randomly distributed N atoms. Therefore, at this electron concentration the homogeneous broadening resulting from the anticrossing interaction is the dominant scattering mechanism that limits the electron mobility. As seen in Fig. 7, at high concentrations the electron mobility calculated from the BAC model is in a very good agreement with experiment. The fact that this good agreement has been obtained without any adjustable parameters provides further support for the BAC description of the electronic structure of InGaAsN alloys.

The results in Fig. 7 show that as the Fermi level moves down away from the original N level with decreasing electron concentration, the mobility continuously increases until E_F drops down to ~0.1 eV, corresponding to an electron concentration of about 4.5×10^{18} cm^{-3}. At lower electron concentrations the mobility starts to decrease, deviating severely from the prediction of Eq. (13). This effect can be attributed to the scattering of the conduction electrons by the random fields caused by the structural and compositional disorder in the alloy. Bonch-Bruevich[28] and Zhumatii[29] have considered the problem of electron transport in a random field in partially disordered semiconductors. They found that as the Fermi level decreases from the degenerate doping regime into the nondegenerate doping regime, the conduction electrons experience increasingly strong scattering from the potential fluctuations. As a result the mobility monotonically decreases with decreasing electron concentration.

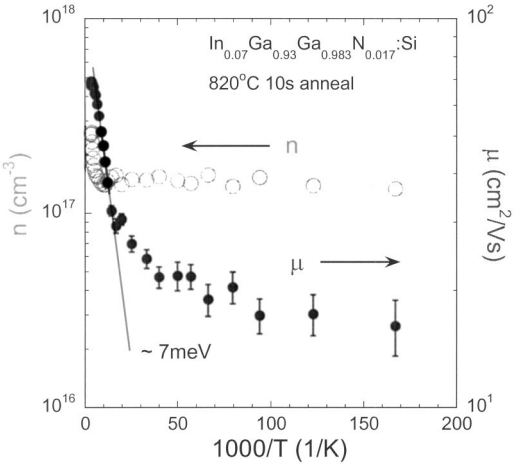

FIG. 8. Free electron concentration and mobility of an 820 °C 10-sec annealed sample measured at temperatures between room temperature and 6 K.

In the case of $In_yGa_{1-y}As_{1-x}N_x$ alloys the main contribution to the potential fluctuations originates from the random N distribution. Calculations of the electron mobility limited by the potential fluctuations are rather difficult, as there is no reliable way to evaluate the shape and size of the scattering potential in this case. An estimate for the electron mobility limited by the random field scattering (μ_2) is shown in Fig. 7. A reasonable agreement with experiment is obtained with a random field distribution with a 30-meV potential depth and a 3-meV/Å potential gradient. Assuming that the potential fluctuations are solely caused by the inhomogeneity of the nitrogen distribution in $In_yGa_{1-y}As_{1-x}N_x$, this potential depth corresponds to approximately a ~18% change in x (i.e., $x = 0.017 \pm 0.003$). The solid curve in Fig. 7 takes into account the contributions of both the level broadening and random alloy scattering effects that limit the mobility [$\mu = 1/(\mu_1^{-1} + \mu_2^{-1})$]. This calculated mobility reproduces the non-monotonic behavior of the mobility measured over two decades of change in electron concentration.

Figure 8 shows the electron concentration and mobility of the 820 °C 10-s annealed sample measured over a wide range of temperatures. The electron concentration stays close to 1.5×10^{17} cm^{-3} for most of this range of temperatures. Similar to the results obtained with Sn-doped InGaAsN alloys reported by Kurtz *et al.*,[22] the mobility shows a thermally activated behavior at relatively high temperatures (>50 K) and becomes only weakly temperature dependent at low temperatures. The mobility activation energy is about 7 meV in the high temperature regime, which is comparable to the activation energy of samples with n between 0.9×10^{17} and 1.5×10^{17} cm^{-3} in Ref. 22. The activated character of the mobility is usually interpreted as a signature of the random field scattering that can be effectively suppressed as free electrons are thermally activated out of the potential at high temperatures.[22]

It should be noted that the band anticrossing model has been successfully used to describe electronic properties of a

broad class of semiconductor materials, the highly mismatched alloys. The BAC effects have been shown to be responsible for the strong band-gap bowing in alloys such as $InP_{1-x}N_x$,[30] $InSb_{1-x}N_x$[31] and $GaSb_{1-x}P_x$ (Ref. 1) (group III-V), and $ZnTe_{1-x}Se_x$,[3] $CdTe_{1-x}O_x$,[32] and $ZnSe_{1-x}O_x$ (Ref. 33) (group II-VI). Accordingly, we expect that the mutual passivation effects should be a general phenomenon observable in all highly mismatched alloys in which substitutional shallow donors and the highly electronegative minority component anions can form nearest-neighbor pairs. Indeed, we have recently shown that Ge-doped $GaAs_{1-x}N_x$ also shows the effect of mutual passivation between Ge_{Ga} donors and N_{As} impurities when annealed at above $\sim$700 °C.[34]

V. CONCLUSIONS

We have studied the mutual passivation phenomenon observed in highly mismatched $In_yGa_{1-y}As_{1-x}N_x$ alloys doped with Si donors. It is shown that upon thermal annealing, Si donors diffuse in the Ga sublattice until forming Si_{Ga}-N_{As} nearest-neighbor pairs. This process results in the mutual passivation of electronic activities of Si as a shallow donor and N as an isovalent impurity. The diffusion-passivation process is analyzed in the context of Si diffusion mediated by Ga vacancies. Monte Carlo simulation has also been performed and shows good agreement with the experimental data. The free electron mobility has been measured and explained on the basis of the electron state broadening caused by the band anticrossing interaction between the N localized states and extended states of the host InGaAs. Results of optical measurements are also presented and discussed. The thermal stability of the mutual passivation effect suggests potential applications in the fabrication of electrical structures by selectively introducing shallow donors and isovalent impurities.

ACKNOWLEDGMENTS

We thank Dr. Hartmut Bracht for helpful discussions. This work was supported by the Director, Office of Science, Office of Basic Energy Sciences, Division of Materials Sciences and Engineering, of the U.S. Department of Energy under Contract No. DE-AC03-76SF00098. J.W. and E.E.H. acknowledge support from U.S. NSF Grant No. DMR-0109844.

*Electronic mail: w_walukiewicz@lbl.gov

[1] J. Wu, W. Shan, and W. Walukiewicz, Semicond. Sci. Technol. **17**, 860 (2002).

[2] K. M. Yu, W. Walukiewicz, J. Wu, J. W. Beeman, J. W. Ager III, E. E. Haller, I. Miotkowski, A. K. Ramdas, and P. Becla, Appl. Phys. Lett. **80**, 1571 (2002).

[3] J. Wu, K. M. Yu, W. Walukiewicz, J. W. Ager III, E. E. Haller, I. Miotkowski, A. K. Ramdas, Ching-Hua Su, I. K. Sou, R. C. C. Perera, and J. D. Denlinger, Phys. Rev. B **67**, 035207 (2003).

[4] W. Walukiewicz, W. Shan, K. M. Yu, J. W. Auger III, E. E. Haller, I. Miotkowski, M. J. Seong, H. Alawadhi, and A. K. Ramdas, Phys. Rev. Lett. **85**, 1552 (2000).

[5] K. M. Yu, W. Walukiewicz, W. Shan, J. W. Ager III, J. Wu, E. E. Haller, J. F. Geisz, D. J. Friedman, J. M. Olson, and Sarah R. Kurtz, Phys. Rev. B **61**, R13 337 (2000).

[6] K. M. Yu, W. Walukiewicz, W. Shan, J. Wu, J. W. Ager III, E. E. Haller, J. F. Geisz, and M. C. Ridgway, Appl. Phys. Lett. **77**, 2858 (2000).

[7] K. M. Yu, Semicond. Sci. Technol. **17**, 785 (2002).

[8] K. M. Yu, W. Walukiewicz, J. Wu, D. Mars, D. R. Chamberlin, M. A. Scarpulla, O. D. Dubon, and J. F. Geisz, Nature Mater. **1**, 185 (2002).

[9] A. Polimeni, G. Baldassarri H. v. , H. M. Bissiri, M. Capizzi, M. Fischer, M. Reinhardt, and A. Forchel, Phys. Rev. B **63**, 201304 (2001).

[10] *Hydrogen in Semiconductors*, edited by J. I. Pankove and N. M. Johnson, Semiconductors and Semimetals, Vol. 34 (Academic, New York, 1991).

[11] W. Walukiewicz, Physica B **302–303**, 123 (2001).

[12] E. F. Schubert, J. B. Stark, T. H. Chiu, and B. Bell, Appl. Phys. Lett. **53**, 293 (1988).

[13] G. Bosker, N. A. Stolwijk, J. Thordson, U. Sodervall, and T. G. Andersson, Phys. Rev. Lett. **81**, 3443 (1998).

[14] Pauling electronegativities of N and As are 3.0 and 2.0, respectively. See Walter Gordy and W. J. Thomas, J. Chem. Phys. **24**, 439 (1956).

[15] The bond strengths for Si-N and Si-P are 470 and 363 kJ/mol, respectively, but values for Si-As is not available. However, we believe from electronegativity arguments that the bond strength of Si-P should be similar to that of Si-As.

[16] D. E. Aspnes, Surf. Sci. **37**, 418 (1973).

[17] S. Yu, U. M. Goesele, and T. Y. Tan, J. Appl. Phys. **66**, 2952 (1989).

[18] T. Ahlgren, J. Likonen, J. Slotte, J. Raeisaenen, M. Rajatora, and J. Keinonen, Phys. Rev. B **56**, 4597 (1997).

[19] J. S. Blakemore, J. Appl. Phys. **53**, R123 (1982).

[20] C. Skierbiszewski, P. Perlin, P. Wisniewski, W. Knap, T. Suski, W. Walukiewicz, W. Shan, K. M. Yu, J. W. Ager, E. E. Haller, J. F. Geisz, and J. M. Olson, Appl. Phys. Lett. **76**, 2409 (2000).

[21] I. Suemune, K. Uesugi, and W. Walukiewicz, Appl. Phys. Lett. **77**, 3021 (2000).

[22] Steven R. Kurtz, A. A. Allerman, C. H. Seager, R. M. Sieg, and E. D. Jones, Appl. Phys. Lett. **77**, 400 (2000).

[23] J. F. Geisz, D. J. Friedman, J. M. Olson, S. R. Kurtz, and B. M. Keyes, J. Cryst. Growth **195**, 401 (1998).

[24] W. Shan, W. Walukiewicz, J. W. Ager III, E. E. Haller, J. F. Geisz, D. J. Friedman, J. M. Olson, and S. R. Kurtz, Phys. Rev. Lett. **82**, 1221 (1999).

[25] C. Skierbiszewski, P. Perlin, P. Wisniewski, T. Suski, J. F. Geisz, K. Hingerl, W. Jantsch, D. E. Mars, and W. Walukiewicz, Phys. Rev. B **65**, 035207 (2001).

[26] J. Wu, W. Walukiewicz, and E. E. Haller, Phys. Rev. B **65**, 233210 (2002).

[27] P. W. Anderson, Phys. Rev. **124**, 41 (1961).

[28] V. L. Bonch-Bruevich, Phys. Status Solidi **42**, 35 (1970).

[29] P. G. Zhumatii, Phys. Status Solidi B **75**, 61 (1976).

[30] K. M. Yu, W. Walukiewicz, J. Wu, J. W. Beeman, J. W. Ager III, E. E. Haller, W. Shan, H. P. Xin, and C. W. Tu, Appl. Phys. Lett. **78**, 1077 (2001).
[31] B. N. Murdin, A. R. Adams, P. Murzyn, C. R. Pidgeon, I. V. Bradley, J.-P. R. Wells, Y. H. Matsuda, N. Miura, T. Burke, and A. D. Johnson, Appl. Phys. Lett. **81**, 256 (2002).
[32] K. M. Yu, W. Walukiewicz, J. Wu, J. W. Beeman, J. W. Ager III, E. E. Haller, I. Miotkowski, A. K. Ramdas, and P. Becla, Appl. Phys. Lett. **80**, 1571 (2002).
[33] W. Shan, W. Walukiewicz, K. M. Yu, J. Wu, J. W. Ager III, E. E. Haller, and Y. Nabetani, Appl. Phys. Lett. **83**, 299 (2003).
[34] K. M. Yu, W. Walukiewicz, J. Wu, W. Shan, J. Beeman, M. A. Scarpulla, O. D. Dubon, M. C. Ridgway, D. E. Mars, D. R. Chamberlin, and J. F. Geisz, Appl. Phys. Lett. **83**, 2844 (2003).